PirB regulates a structural substrate for cortical plasticity

Maja Djurisic[a,1], George S. Vidal[a], Miriam Mann[b,2], Adam Aharon[c], Taeho Kim[a], Alexandre Ferrao Santos[b], Yi Zuo[c], Mark Hübener[b], and Carla J. Shatz[a,1]

[a]Bio-X, James H. Clark Center, Stanford University, Stanford, CA 94305; [b]Max Planck Institute of Neurobiology, D-82152 Martinsried, Germany; and [c]Molecular, Cell and Developmental Biology, University of California, Santa Cruz, CA 95064

Contributed by Carla J. Shatz, November 10, 2013 (sent for review September 28, 2013)

Experience-driven circuit changes underlie learning and memory. Monocular deprivation (MD) engages synaptic mechanisms of ocular dominance (OD) plasticity and generates robust increases in dendritic spine density on L5 pyramidal neurons. Here we show that the paired immunoglobulin-like receptor B (PirB) negatively regulates spine density, as well as the threshold for adult OD plasticity. In PirB$^{-/-}$ mice, spine density and stability are significantly greater than WT, associated with higher-frequency miniature synaptic currents, larger long-term potentiation, and deficient long-term depression. Although MD generates the expected increase in spine density in WT, in PirB$^{-/-}$ this increase is occluded. In adult PirB$^{-/-}$, OD plasticity is larger and more rapid than in WT, consistent with the maintenance of elevated spine density. Thus, PirB normally regulates spine and excitatory synapse density and consequently the threshold for new learning throughout life.

visual cortex | adult plasticity | LTP | LTD | circuit connectivity

Experience generates both functional and structural changes in neural circuits. The learning process is robust at younger ages during developmental critical periods and continues, albeit at a lower level, into adulthood and old age (1–3). For example, young barn owls exposed to horizontally shifting prismatic spectacles can adapt readily to altered visual input, but adult owls cannot. The experience in the young owls results in a rearranged audiovisual map in tectum that is accompanied by ectopic axonal projections (1). Experience-dependent structural changes have also been observed in the mammalian cerebral cortex. Enriched sensory experience or motor learning are both associated with an increase in dendritic spine density, and a morphological shift from immature thin spines to mushroom spines which harbor larger postsynaptic densities (PSDs) and stronger synapses (4–7). On the flip side, bilateral sensory deprivation induces spine loss (8, 9). Abnormal sensory experience also results in structural modification of inhibitory synapses and circuitry that is temporally and spatially coordinated with changes in excitatory synapses on dendritic spines (10–13).

These experience-driven spine changes are thought to involve synaptic mechanisms of long-term potentiation (LTP) and long-term depression (LTD). In hippocampal slices, induction of LTP causes new spines to emerge, as well as spine head enlargement on existing spines (14–16); induction of LTD results in rapid spine regression (14, 17). Importantly, the emergence or regression of spines starts soon after the induction of LTP or LTD, suggesting that these structural changes underlie the persistent expression of long-term plasticity (14, 17).

Little is known about molecular mechanisms that restrict experience-dependent plasticity at circuit and synaptic levels and connect it to spine stability. Paired Ig-like receptor B (PirB), a receptor expressed in cortical pyramidal neurons, is known to limit ocular dominance (OD) plasticity both during the critical period and in adulthood (18). PirB binds major histocompatibility class I (MHCI) ligands, whose expression is regulated by visual experience and neural activity (19–21) and thus could act as a key link connecting functional to structural plasticity. If so, mice lacking PirB might be expected to have altered synaptic plasticity rules on the one hand and changes in the density and stability of dendritic spines on the other.

Results

Dendritic Spine Density in PirB$^{-/-}$ Mice Is Elevated and Is Insensitive to Effects of Visual Deprivation. Previous imaging studies show that a period of monocular deprivation (MD) generates a net increase in spine density on L5 apical dendrites in visual cortex; this increase is stable and thought to act as a structural substrate for enhanced OD plasticity following a second MD in adulthood (2). To investigate whether PirB regulates dendritic spine density in visual cortex, PirB knockout mice (PirB$^{-/-}$) (18) were crossed to the YFP-H line in which a subset of L5 pyramidal cells expresses YFP (22). The breeding strategy ensured that both PirB$^{-/-}$; YFP^{+} and WT; YFP^{+} were littermates on the same genetic background.

A massive increase in spine density on the apical dendrites of L5 pyramidal neurons was detected in the binocular zone of visual cortex in normally reared juvenile PirB$^{-/-}$ mice: 175% of the WT levels at P30, during the critical period (Fig. 1 *A–C*, and *H*). In visual cortex of WT mice, 3 d of MD (P27–P30) generates a 50% increase in spine density (Fig. 1 *B, D*, and *H*); a similar but smaller spine density increase has been observed previously following 8-d MD in adult WT visual cortex (2). In contrast to WT, spine density following 3-d MD in PirB$^{-/-}$ mice does not increase beyond the already high levels observed in normally

Significance

Learning and memory are mediated by changes in synaptic structure and circuit connectivity; these changes are known as "synaptic plasticity." In the normal brain, the amount of plasticity is fine tuned by regulating a balance between synaptic strengthening and weakening, both in a positive and a negative direction. Here we report that paired immunoglobulin-like receptor B (PirB), an innate immune receptor expressed by neurons, acts as a robust negative regulator of structural substrates for plasticity in visual cortex. Without PirB, there are excessive numbers of spines, accompanied by a shift in Hebbian plasticity favoring synaptic strengthening. These results suggest that PirB regulates spine density in cortex and imply that blocking PirB function could enhance cognition or recovery from injury.

Author contributions: M.D., Y.Z., M.H., and C.J.S. designed research; M.D., G.S.V., M.M., A.A., T.K., and A.F.S. performed research; M.D., G.S.V., and M.M. analyzed data; M.D. and C.J.S. wrote the paper; and Y.Z. and M.H. supervised collaborative experiments.

The authors declare no conflict of interest.

[1]To whom correspondence may be addressed. E-mail: djurisic@stanford.edu or cshatz@stanford.edu.

[2]Present address: Technical University Munich, Wissenschaftszentrum Weihenstephan, 85354 Freising, Germany.

This article contains supporting information online at www.pnas.org/lookup/suppl/doi:10.1073/pnas.1321092110/-/DCSupplemental.

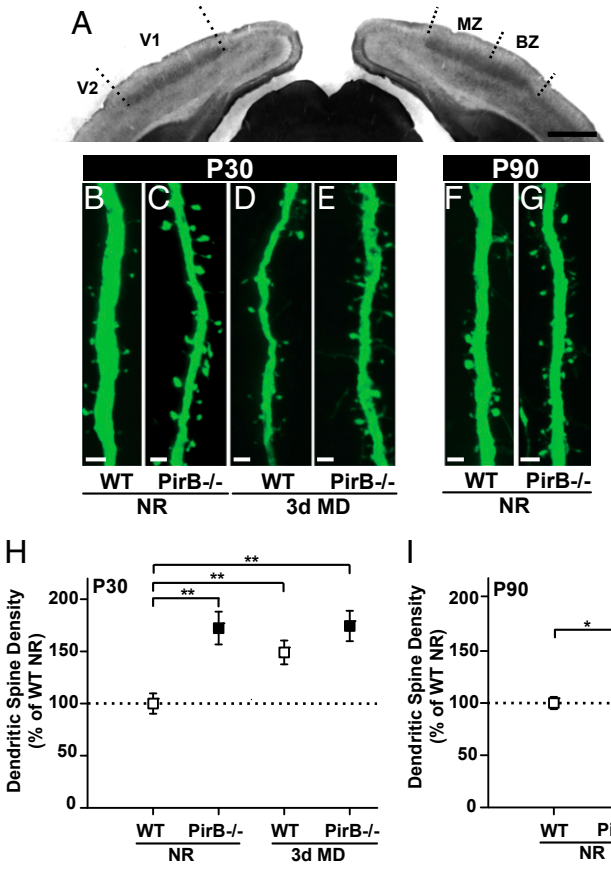

Fig. 1. Dendritic spine density is elevated in PirB$^{-/-}$ binocular zone of primary visual cortex. (*A*) Low-power brightfield image of AchE histochemical stain labeling extent of V1: thalamo-cortical fibers terminating in L4 of V1 are AchE positive; V1-primary and V2-secondary visual cortex (BZ, binocular zone). (*B* and *C*) Example images of L5 pyramidal neuron apical dendrites from normally reared (NR) WT vs. PirB$^{-/-}$ at P30. (*D* and *E*) WT vs. PirB$^{-/-}$ after 3 d of monocular visual deprivation (3-d MD) from P27 to P30. (*F* and *G*) NR WT vs. PirB$^{-/-}$at P90. (*H*) Plot showing 75% increase in spine density at P30 in NR PirB$^{-/-}$ vs. NR WT (0.87 ± 0.08 spines/μm; n = 17/8 vs. 0.50 ± 0.05 spines/μm; n = 13/8; P = 0.001). After 3-d MD, total spine density increases ~50% in WT mice (0.75 ± 0.06 spines/μm; n = 13/5; P = 0.003). No additional increase in spine density in PirB$^{-/-}$ mice after 3-d MD (0.88 ± 0.07 spines/μm; n = 12/6; P = 1.00). (*I*) In adult visual cortex (P90), total spine density is ~43% greater in NR PirB$^{-/-}$ relative to NR WT: WT (1.23 ± 0.07 spines/μm; n = 21/6) vs. PirB$^{-/-}$ (1.77 ± 0.16 spines/μm; n = 21/7, P = 0.02). (*H* and *I*) Spine density normalized to NR WT at appropriate age. [Calibration bars: (*A*) 1 mm, (*B–F*) 2 μm.] Mean ± SEM; n = cells/mice. *P < 0.05, **P < 0.01; Kruskal-Wallis followed by U test (Table S1).

reared PirB$^{-/-}$ mice (Fig. 1 *C, E*, and *H*). In other words, spine density in PirB$^{-/-}$ mice is saturated before monocular deprivation.

The elevated spine density on L5 apical dendrites in juvenile PirB$^{-/-}$ visual cortex persists into adulthood. At P90 in normally reared PirB$^{-/-}$ mice, spine density is 43% greater than in WT (Figs. 1 *F, G*, and *I*).

Dendritic Spine Motility Is Decreased in the Absence of PirB. Previous in vivo imaging experiments suggest that spine density is inversely correlated with spine dynamics and persistence (23). Thus, we investigated if dendritic spine motility on L5 neurons in PirB$^{-/-}$ mice is altered in normally reared and in mice after 3-d MD, relative to WT (24, 25). Spine dynamics along L5 apical dendrites located within the binocular zone were measured using in vivo two-photon imaging through a thinned skull (6) of WT or PirB$^{-/-}$ carrying the YFP-H transgene (Fig. 2 *A–E*). There is a significant ~25% decrease in spine motility in normally reared PirB$^{-/-}$ mice compared with WT (Fig. 2*E*). Similar results were obtained from two-photon imaging of spines in vitro in acutely isolated brain slices (Fig. S1). These experiments imply that PirB signaling normally enhances spine motility. The lower motility of spines in normally reared PirB$^{-/-}$ mice suggests that they are more stable, which in turn could make spines more resistant to elimination, thereby accounting for the higher spine density detected on apical dendrites of L5 pyramidal neurons in mutant visual cortex (Fig. 1).

Studies have shown that sensory deprivation causes a decrease in spine motility (25); moreover, learning is ultimately associated with spine stabilization and an overall decrease in turnover rates. As noted above (Fig. 1*H*), spine density in PirB$^{-/-}$ mice does not change with MD, raising the question of whether spine motility is also resistant to the effects of deprivation. Spine motility was measured in the binocular zone contralateral to the derived eye at the end of 3-d MD (P27–P30). In WT visual cortex, spine

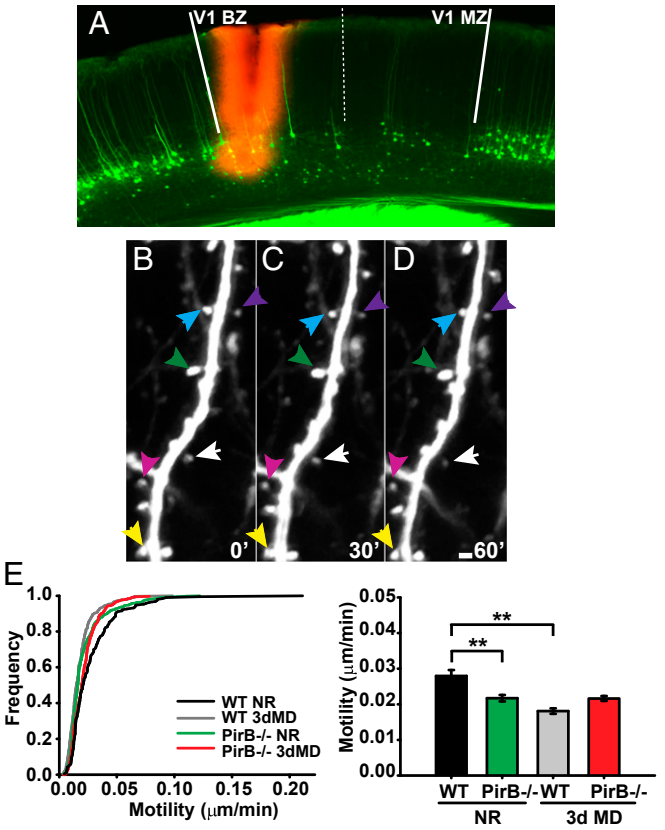

Fig. 2. Dendritic spine motility in vivo is lower in PirB$^{-/-}$ visual cortex. (*A*) Example fluorescent micrograph of a coronal section cut following in vivo spine motility imaging session. YFP (green) labels L5 pyramidal cells in WT vs. PirB$^{-/-}$ mice crossed to YFP-H line. DiI injection (red) confirms imaging location within V1 binocular zone (V1 BZ, binocular zone; MZ, monocular zone); DiI needle track is visible. The example image is from a WT mouse brain after 3-d MD. (*B–D*) Maximum intensity projection images of L5 apical dendrites from Z-stacks obtained by two-photon microscopy at 0, 30, and 60 min into imaging session. Color-coded arrowheads point to same spines at all three time points. (Scale bar, 2 μm.) Example dendrite is from a normally reared PirB$^{-/-}$. (*E*) Spine motility measurements in NR and after 3-d MD. (*Left*) Cumulative distribution plots of all data points. (*Right*) Bar graphs of mean ± SEM. WT NR (n = 190) vs. PirB$^{-/-}$ NR (n = 366; P < 0.001); WT 3-d MD (n = 255) vs. PirB$^{-/-}$ 3-d MD (n = 293; P < 0.001); PirB$^{-/-}$ NR vs. PirB$^{-/-}$ 3-d MD, P = 0.001. n = number of spines, from four WT NR, five PirB$^{-/-}$ NR, four WT 3-d MD, and seven PirB$^{-/-}$ 3-d MD mice. Kruskal-Wallis, followed by pairwise U test (Fig. S1 and Table S1).

motility dropped by ~35% averaged over all spine types (Fig. 2*E*). The lower motility of these spines following MD in WT correlates well with the observed 50% net increase in spine density found after 3-d MD (Fig. 1). These observations are consistent with the idea that activity from the open eye drives stabilization of newly formed or rearranged connections in WT visual cortex.

In contrast, in PirB$^{-/-}$ mice following 3-d MD, there is no obvious change in spine motility averaged across all spine types (Fig. 2*E*). In sum, in vivo imaging experiments of spine motility further support the idea that dendritic spines in neurons lacking PirB are more stable and therefore could constitute a readily available anatomical substrate enabling rapid and enhanced ocular dominance plasticity.

Miniature Excitatory Postsynaptic Current Frequency Is Increased in L5 and L2/3 Pyramidal Neurons in the Visual Cortex of PirB$^{-/-}$ Mice. To examine whether the increased spine density on apical dendrites of L5 neurons in PirB$^{-/-}$ mice (Fig. 1) is accompanied by an increase in the number of functional excitatory synaptic inputs, spontaneous miniature excitatory postsynaptic potentials (mEPSCs) were recorded from L5 pyramidal cells in slices of visual cortex from P27–P32 mice (Fig. 3). In addition, recordings were made from L2/3 pyramidal neurons because PirB is expressed in this layer as well (18). L5 mEPSCs recorded in PirB$^{-/-}$ slices are significantly increased in frequency (146%) over WT (Fig. 3 *A* and *B*). L2/3 mEPSC frequency is similarly increased (158%) (Fig. 3 *D* and *E*). On the other hand, there is no change in mEPSC amplitude in neurons in either cortical layer (Fig. 3 *C* and *F*). The increase in frequency but not amplitude in L5 PirB$^{-/-}$ cortical neurons is consistent with the observed elevation in spine density and implies that there is a functional enhancement of excitatory connectivity. Because this physiological change is also observed in layer 2/3 neurons, it is highly likely that they too undergo a spine density increase.

LTP Is Enhanced and LTD Is Impaired at L4-L2/3 Synapses in PirB$^{-/-}$ Mouse Visual Cortex. The induction paradigm for LTD is known to result in a rapid loss of spines, whereas that for LTP generates a rapid spine increase (14). If spines are already at maximum density and are more resistant to elimination, as they appear to be in PirB$^{-/-}$ visual cortex, then it is possible that elementary mechanisms of synaptic plasticity might be abnormal. One possibility is that LTP might be occluded using standard LTP-inducing protocols. We therefore examined LTP, as well as LTD, at L4 to L2/3 synapses using field recordings in visual cortical slices at P27–P32 (Fig. 4). Unexpectedly, the magnitude of LTP is almost twice as large in PirB$^{-/-}$ vs. WT 60 min after induction with theta-burst stimulation (TBS) (Fig. 4 *A* and *B*). Moreover, LTD at the L4 to L2/3 synapse in PirB$^{-/-}$ mice cannot be elicited using standard low-frequency stimulation (LFS), whereas in WT littermates in the same protocol generated the expected robust synaptic depression (40% below baseline; Fig. 4 *C* and *D*) (26). The absence of LFS-induced LTD is consistent with the resistance of dendritic spines to undergo elimination, a well-known correlate of synaptic weakening (14, 17, 27). The presence of enhanced LTP implies that the additional spines present in PirB$^{-/-}$ mice represent readily available synaptic substrate that can strengthen further.

In Adult PirB$^{-/-}$ Mice, 3-d Period of MD Generates a Large OD Shift. The increase in spine density in both juvenile and adult PirB$^{-/-}$ cortex could contribute to the enhanced OD plasticity reported previously (18). Furthermore, given the increase in LTP and deficient LTD seen above, we would predict that OD plasticity in PirB$^{-/-}$ mice is mostly carried by open eye strengthening, whereas closed eye weakening might be decreased compared with WT (28, 29). Two independent methods, in vivo intrinsic signal imaging (30) and induction of the immediate early gene Arc (18, 31), were used to assess the effect of a 3-d period of monocular eye closure (MD) on OD plasticity in adult (P90) PirB$^{-/-}$ or WT mice. For in vivo intrinsic signal imaging experiments, the strength of cortical responses to visual stimulation of the open vs. the deprived eye was imaged in the hemisphere contralateral to the deprived eye (Fig. 5*A* and Fig. S2). In adult WT mice, 3-d MD is too short to result in open eye strengthening relative to response strength in normally reared mice, similar to previous observations (32–34). Weakening of cortical responses to the closed (contralateral) eye can be detected in WT after 3-d MD (Fig. 5*B*). In striking contrast, in adult PirB$^{-/-}$ mice, open eye responses double in strength after just 3-d MD. At the same time, there is no significant decrease in response strength after deprived (contralateral) eye stimulation (Fig. 5*B*).

Open eye strengthening was also measured using immediate early gene induction of Arc mRNA (Fig. 5 *C* and *D* and Fig. S2) (31).The functional representation of the open (ipsilateral) eye is significantly increased in P90 PirB$^{-/-}$ after 3-d MD, whereas no significant increase is detected in WT mice, relative to normally reared cohorts of both genotypes. This observation confirms the results from intrinsic signal imaging and demonstrates that the enhanced OD plasticity previously reported in adult PirB$^{-/-}$

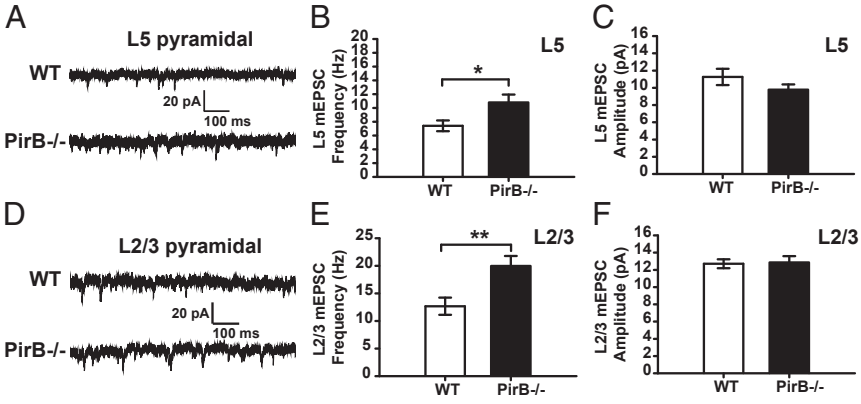

Fig. 3. Increased frequency of mEPSCs recorded from L5 and L2/3 pyramidal cells in PirB$^{-/-}$ visual cortex. (*A*) Example traces of L5 mEPSC from WT (*Upper*) vs. PirB$^{-/-}$ mice (*Lower*). (*B*) L5 mEPSC frequency in WT ($n = 5$) vs. PirB$^{-/-}$ ($n = 7$; $P = 0.03$). (*C*) L5 mEPSC amplitude in WT ($n = 5$) vs. PirB$^{-/-}$ ($n = 7$; $P = 0.20$). (*D*) Example traces of L2/3 mEPSC from WT vs. PirB$^{-/-}$ mice. (*E*) L2/3 mEPSC frequency in WT (n= 15) vs. PirB$^{-/-}$ ($n = 18$; $P = 0.002$). (*F*) L2/3 mEPSC amplitude in WT ($n = 15$) vs. PirB$^{-/-}$ ($n = 18$; $P = 0.96$). n = cells; *U* test (Table S1).

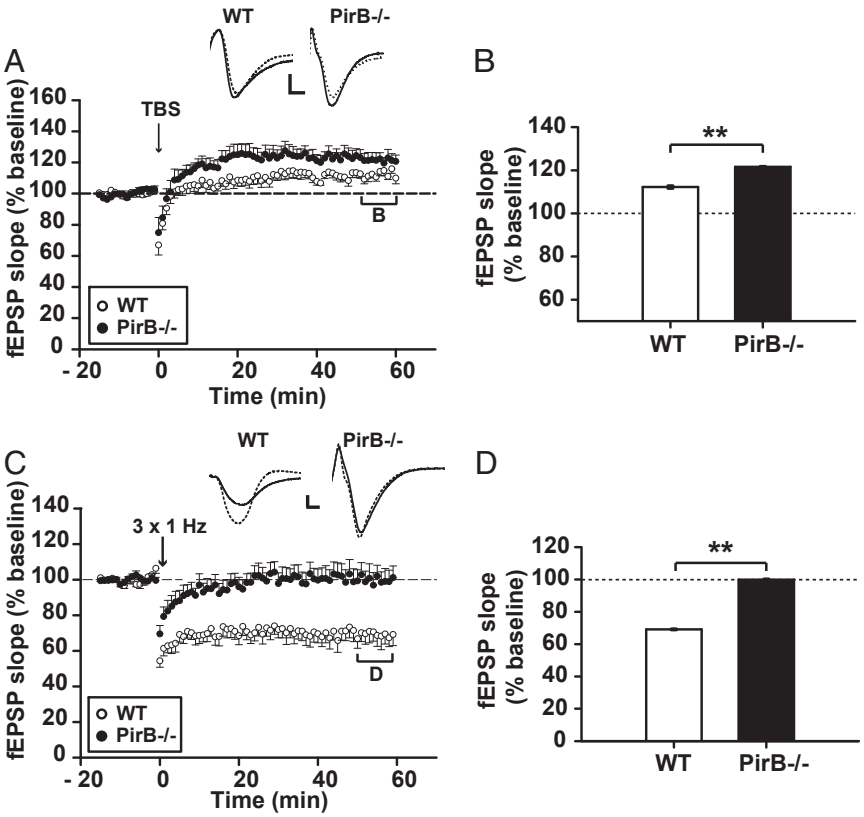

Fig. 4. Enhanced LTP and impaired LTD at L4-2/3 synapse in PirB$^{-/-}$ visual cortex. (*A*) LTP in WT and PirB$^{-/-}$, measured as an increase in the slope of the field excitatory postsynaptic potential (fEPSP) after TBS relative to baseline; PirB$^{-/-}$ (n = 14 slices/11 mice) vs. WT (n = 13 slices/6 mice); "B" marks data points used for 10-min average shown in *B*. (*Insets*) Example fEPSP traces from WT and PirB$^{-/-}$ mice before (dotted traces) and after (solid traces) LTP was induced with TBS. Each trace is an average of 30 single trials. (*B*) Bar graphs showing fEPSP slope measured 60 min after TBS induction. (*C*) LTD measured as a decrease in fEPSP slope, relative to baseline, after LFS protocol. PirB$^{-/-}$ (n = 16 slices/7 mice) vs. WT mice (n = 12 slices/5 mice). (*Inset*) Example fEPSP traces from WT and PirB$^{-/-}$ mice before (dotted traces) and after (solid traces) LTD was induced. Each trace is average of 30 single trials. "D" marks data points used for 10-min average in *D*. (*D*) Plot of fEPSP slope measured 60 min after LFS induction. (*B* and *D*) Each bar graph is the average of 10 min of recording and then averaged across all slices for each genotype. (*A* and *C*) Vertical calibration bar = 0.2 mV, horizontal = 2 ms. (*B* and *D*) **P < <0.01, t test (Table S1).

visual cortex can be engaged with an extremely brief period of just 3-d MD (18).

Discussion

A major finding of this study is that the increased spine density and decreased spine motility on L5 cortical pyramidal neurons can explain enhanced sensory-driven plasticity present in visual cortex of PirB$^{-/-}$ mice. We observed a dramatic (>50%) increase in spine density on the apical dendrites of L5 pyramidal neurons, which is also accompanied by a significant increase in functional excitatory synapses on L2/3 and L5 pyramidal cells, both in juveniles and in adults. The increased OD plasticity following MD in PirB$^{-/-}$ visual cortex, measured by intrinsic signal imaging or by Arc mRNA induction, occurs primarily via rapid strengthening of the open eye. At the cellular level, this change is accompanied by enhanced LTP and absent LTD at L4 to L2/3 synapses, correlating well not only with greater open eye strengthening and absence of closed eye weakening but also with the excessive numbers of spines present in PirB$^{-/-}$ mice. These observations imply that PirB normally facilitates activity-dependent spine regression. The coupling of spine density increases to a shift in synaptic plasticity toward LTP and away from LTD as shown here also implies that Hebbian synaptic plasticity in visual cortex may be regulated by spine density.

PirB Regulates a Structural Substrate for Plasticity in Visual Cortex. Studies have shown that learning or sensory deprivation initially results in increases in spine turnover and motility in dendrites of neurons located in a variety of cortical areas, eventually resulting in a net increase in spine number when examined at later times (2, 24, 35). In motor cortex, learning a novel task increases the net number of spines on apical dendrites of L5 neurons by 5% (6). Enriched environmental rearing results in new spine formation by about 5% above baseline (36). In visual cortex, MD performed in adult mice causes an 8% increase in the number of spines on apical dendrites of L5 neurons (2). In all these cases, a relatively small addition of spines is strongly correlated with, and thought to mediate, better task performance or lower threshold for plasticity later in life. Similar increases in spine turnover, density, and synaptic strength associated with learning have also been seen in other systems including the song system in birds (35). However, in none of these systems is it known how these changes in spine density are regulated at the molecular level. Our findings suggest that PirB contributes to this process.

It was unexpected to find that LTP is enhanced in PirB$^{-/-}$ mice. Given that spine density appears to be saturated in these mice, we might have expected LTP to be occluded. However, in hippocampus, increases in the size and function of preexisting spines are also known to accompany potentiation of AMPA receptor synaptic currents (16). In mouse visual cortex, the size of the spine head closely correlates with the size of the postsynaptic density, i.e., the larger the spine the stronger the synapse (37). Thus, although we cannot exclude a possibility that in PirB$^{-/-}$, spine formation might also be enhanced and serve as an

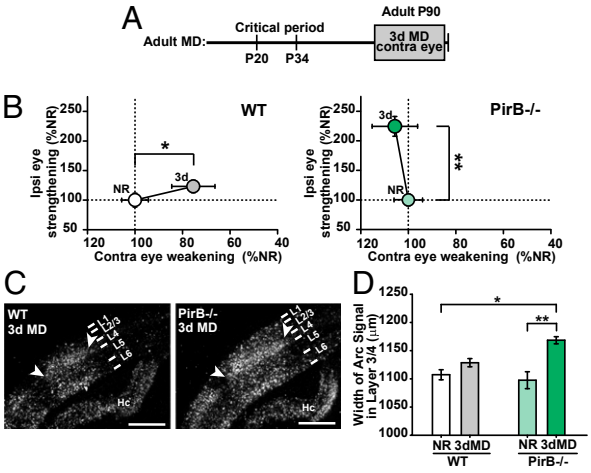

Fig. 5. Brief monocular deprivation results in significant open eye strengthening and OD plasticity in adult PirB$^{-/-}$ but not WT mice. (*A*) Experimental paradigm for 3 d of MD in adult mice. (*B*) Intrinsic signal imaging experiment showing ipsilateral (Ipsi; open) eye strengthening plotted against contralateral (Contra; closed) eye weakening; response strengths are normalized to eye-specific response strength in normally reared (NR) condition for each genotype. WT: open eye strengthening is not detected following 3-d MD; contra-eye weakening is present: Ipsi: NR ($n = 8$) vs. 3-d MD ($n = 7$, $P = 0.121$), Contra: NR ($n = 8$) vs. 3-d MD ($n = 7$, $P = 0.014$). In PirB$^{-/-}$, 3-d MD significantly increases open eye response and does not generate weakening of the closed (Contra) eye: Ipsi: NR ($n = 8$) vs. 3-d MD ($n = 6$, $P = 0.001$), Contra: NR ($n = 8$) vs. 3-d MD ($n = 6$, $P = 0.662$). *$P < 0.05$, **$P < 0.01$; *U* test. (*C* and *D*) Open (Ipsi) eye strengthening following 3-d MD using Arc mRNA induction method. (*C*) Example micrographs of isotopic in situ hybridization for Arc mRNA in WT (*Left*) or PirB$^{-/-}$ (*Right*) mouse visual cortex ipsilateral to the open eye after 3-d MD. Arrowheads mark the region of Arc mRNA induction within the BZ in layer 3/4. Note wider zone of hybridization signal in PirB$^{-/-}$. Cortical layers are indicated at right; Hc, hippocampus. (Scale bar, 300 μm.) (*D*) Graph of the width of Arc mRNA in situ hybridization signal measured in L3/4 binocular zone induced by stimulation of Ipsi (open) eye in WT vs. PirB$^{-/-}$. In PirB$^{-/-}$ cortex, significant widening of Arc mRNA signal is detected after 3-d MD but is not present in WT. WT NR ($n = 12$) vs. 3-d MD ($n = 12$); $P = 0.68$. PirB$^{-/-}$ NR ($n = 12$) vs. 3-d MD ($n = 11$); $P < 0.001$. n = mice. Weighted means ± SEM were plotted. *$P < 0.05$, **$P < 0.01$; one-way ANOVA, post hoc Tukey, with stratified bootstrap sampling (Fig. S2 and Table S1).

additional mechanism for increased LTP, the larger LTP observed in PirB$^{-/-}$ can be explained by proposing that existing supernumerary spines are still able to undergo spine head and PSD enlargement.

The eye-specific changes observed here in OD plasticity in adult PirB$^{-/-}$ mice also correlate well with enhanced LTP and impaired LTD in L2/3 of visual cortex. The absence of closed eye response weakening following MD is consistent with a deficiency in synaptic LTD in L2/3, whereas rapid and larger than normal open eye response strengthening can be attributed to the immediate availability of more synapses that are able to strengthen in PirB$^{-/-}$ than in WT visual cortex (28, 29). The loss of LFS-induced LTD is reminiscent of the occlusion of LTD following MD (28), as if in PirB$^{-/-}$ mice cortical circuits have already been conditioned by prior experience.

PirB, a Receptor Linking Synaptic Structure and Plasticity in Mouse Visual Cortex. Our findings imply that PirB is part of a molecular mechanism that regulates the encoding of experience-dependent plasticity into stable structural change. In this context, it is possible that PirB is involved with the Nogo/NgR system to regulate adult OD plasticity (38), consistent with the observation that PirB binds NogoA (39). However, although we find significant spine density increases in PirB$^{-/-}$ adult visual cortex along with increased spine stability and LTP, in adult NgR$^{-/-}$ somatosensory cortex only spine turnover is enhanced, suggesting lower spine stability than normal; no frank change in synaptic density was observed in somatosensory cortex in these mice (40). Another receptor, DR6, was also recently found to regulate structural plasticity in adult cortex: horizontal axons of L2/3 pyramidal and inhibitory neurons in somatosensory cortex of adult DR6$^{-/-}$ mice fail to prune following whisker plucking, and bouton density is increased (13). In view of our findings, we would expect DR6$^{-/-}$mice to have systems-level changes in somatosensory and even OD plasticity. In the future, it will be revealing to examine the direct and indirect interactions between these three receptors.

In the context of a sliding synaptic modification threshold that would permit synaptic weights to change with experience (29), PirB, by negatively regulating spine and synapse stability, might normally act to prevent Hebbian synaptic mechanisms from sliding too far toward synaptic strengthening. In the extreme, hyperactivation of PirB signaling would be expected to slide plasticity too far toward synaptic weakening, leading to synapse elimination. This excessive synaptic weakening is exactly what is seen in Alzheimer's disease (AD) and is consistent with our recent discovery that PirB is a high affinity receptor for β-amyloid and that disease phenotypes in AD model mice, including lack of OD plasticity (41) and enhanced LTD, can be rescued to WT by deleting PirB (42). Together, these experiments demonstrate a tight coupling of synaptic structure to synaptic plasticity mechanisms and argue for a key role for PirB in this process.

Materials and Methods

Experimental Animals. Experiments were performed using WT and PirB$^{-/-}$ mice all on the same mixed (C57BL/6 × SV/ 129J) genetic background and were carried out in accordance with the guidelines of the local government (Regierung von Oberbayern) and the Max Planck Society, Harvard University, and Stanford University Institutional Animal Care and Use Committees.

Monocular Visual Deprivation. MD was performed on juvenile (P27–P30) or adult mice (P90–P110) for 3 d as described previously (32).

For monocular enucleation (see below), mice were anesthetized with isofluorane, one eye was removed, and pieces of gelfoam were inserted into the cavity. A drop of Vetbond (3M) was put on eyelids to prevent reopening.

Dendritic Spine Imaging and Spine Density Analysis. ***Generating PirB$^{-/-}$ YFP^{+} mice.*** The YFP-H line from Jackson Laboratories [B6.Cg-Tg(Thy1-YFPH)2Jrs/J] was crossed to the PirB$^{-/-}$ line. YFP-positive F_1 offspring, all heterozygous for PirB, was used to set-up a breeding colony. F_2 offspring provided WT and PirB$^{-/-}$ littermates, which were YFP^{+} and were used in experiments to determine dendritic spine density. Juvenile females and males and adult males were used.

Dendritic spine density measurements. Brains from normally reared (P30 and P90) and mice after 3-d MD (P27–P30) were fixed via transcardial perfusion with 4% (wt/vol) paraformaldehyde in PBS. The hemisphere contralateral to the deprived eye was sectioned coronally, and brain sections were used for fluorescence microscopy of YFP^{+} neurons. Sections were cut at 150 μm and were interleaved with 25-μm sections used for detecting V1 and binocular zone with an acetylcholine esterase (AchE) stain.

Distal apical dendrites of L5 neurons labeled with YFP were then imaged with a confocal microscope (Leica Microsystems) using a 63× oil immersion objective and 8× zoom. High-resolution images (1,024 × 1,024 pixels, 0.03 μm/pixel, 0.16- to 0.2-μm *z* axis resolution) of apical tufts and the primary dendritic shaft immediately below the main branching of the dendrite (approximate layer 2/3 border) were used in the analysis. The analysis was done blind to the genotype and vision deprivation condition.

Dendritic Spine Motility Measurements. ***In vivo transcranial imaging.*** The procedure for transcranial two-photon imaging has been described previously (6). See *SI Materials and Methods* for details.

Data quantification. All analysis of spine dynamics was done manually using ImageJ software, blind with regard to genotype and experimental condition. Dendritic segments were identified from 3D image stacks selected for S/N > 4, providing high enough contrast to detect both location and lengths of spines. Detailed description of image stack analysis and motility index calculation is in *SI Materials and Methods*.

Visual Cortex Slice Physiology. ***Brain slice preparation.*** Acute brain slices were prepared using standard procedures, taking care to prevent detrimental effects of excitotoxicity and hypoxia.

Single-cell mEPSC recordings. The whole-cell patch-clamp technique was used to record spontaneous synaptic events from pyramidal cells in visual cortex slices. Measurement conditions and isolation of mEPSCs were done using previously established protocols.

Visual cortex synaptic plasticity. L4 to L2/3 LTP and LTD experiments were performed using extracellular field recordings.

See *SI Materials and Methods* for detailed recording conditions and analysis of single cell events and synaptic plasticity experiments.

Optical Imaging of Intrinsic Signals. Intrinsic signal imaging was used to investigate changes in response strength in the binocular zone of visual cortex resulting from MD (32). The visual cortex was illuminated with monochromatic light at 707 nm, and intrinsic signals were recorded with a slow scan charge-coupled device (CCD) camera (12 bit, 384 × 288 pixels, ORA 2001; Optical Imaging). Anesthesia, visual stimulation, and data acquisition are described in *SI Materials and Methods*.

Arc Induction, Arc In Situ Hybridization, and Analysis. One eye (the deprived eye in MD mice), was enucleated 24 h before visual stimulation, and mice were put in total darkness. Mice were returned to a lighted environment for 30 min in the alert condition. After light exposure, mice received an overdose of sodium pentobarbital (1 mg/g body weight); brains were removed, flash-frozen in M-1 mounting medium (ThermoShandon), and sectioned coronally at 16 μm for in situ hybridization. In situ hybridization was performed as described previously (31). Images were taken using dark-field optics with a cooled CCD camera (SPOT; Diagnostic instruments). Before analysis, sections were visually screened. Analysis was done blind to condition. See *SI Materials and Methods* for detail.

ACKNOWLEDGMENTS. We thank Dr. Thorsten Naserke for help in the early stages of dendritic spine analysis and Drs. Matt Scott and Manny Lopez for access and help with the confocal microscope. This work was supported by National Institutes of Health Grant EY02858 and the G. Harold and Leila Y. Mathers Charitable Foundation (to C.J.S.), National Institute of Mental Health Grant R01MH09449 (to Y.Z.), a Regina Casper Stanford Graduate fellowship (to G.S.V.), and the Max Planck Society (M.M. and M.H.).

1. Linkenhoker BA, von der Ohe CG, Knudsen EI (2005) Anatomical traces of juvenile learning in the auditory system of adult barn owls. *Nat Neurosci* 8(1):93–98.
2. Hofer SB, Mrsic-Flogel TD, Bonhoeffer T, Hübener M (2009) Experience leaves a lasting structural trace in cortical circuits. *Nature* 457(7227):313–317.
3. Zuo Y, Yang G, Kwon E, Gan WB (2005) Long-term sensory deprivation prevents dendritic spine loss in primary somatosensory cortex. *Nature* 436(7048):261–265.
4. Parnavelas JG, Globus A, Kaups P (1973) Continuous illumination from birth affects spine density of neurons in the visual cortex of the rat. *Exp Neurol* 40(3):742–747.
5. Holtmaat A, Wilbrecht L, Knott GW, Welker E, Svoboda K (2006) Experience-dependent and cell-type-specific spine growth in the neocortex. *Nature* 441(7096):979–983.
6. Xu T, et al. (2009) Rapid formation and selective stabilization of synapses for enduring motor memories. *Nature* 462(7275):915–919.
7. Fu M, Yu X, Lu J, Zuo Y (2012) Repetitive motor learning induces coordinated formation of clustered dendritic spines in vivo. *Nature* 483(7387):92–95.
8. Valverde F (1967) Apical dendritic spines of the visual cortex and light deprivation in the mouse. *Exp Brain Res* 3(4):337–352.
9. Montey KL, Quinlan EM (2011) Recovery from chronic monocular deprivation following reactivation of thalamocortical plasticity by dark exposure. *Nat Commun* 2(317):1–8.
10. Chen JL, et al. (2012) Clustered dynamics of inhibitory synapses and dendritic spines in the adult neocortex. *Neuron* 74(2):361–373.
11. Chen JL, et al. (2011) Structural basis for the role of inhibition in facilitating adult brain plasticity. *Nat Neurosci* 14(5):587–594.
12. van Versendaal D, et al. (2012) Elimination of inhibitory synapses is a major component of adult ocular dominance plasticity. *Neuron* 74(2):374–383.
13. Marik SA, Olsen O, Tessier-Lavigne M, Gilbert CD (2013) Death receptor 6 regulates adult experience-dependent cortical plasticity. *J Neurosci* 33(38):14998–15003.
14. Nägerl UV, Eberhorn N, Cambridge SB, Bonhoeffer T (2004) Bidirectional activity-dependent morphological plasticity in hippocampal neurons. *Neuron* 44(5):759–767.
15. Engert F, Bonhoeffer T (1999) Dendritic spine changes associated with hippocampal long-term synaptic plasticity. *Nature* 399(6731):66–70.
16. Matsuzaki M, Honkura N, Ellis-Davies GC, Kasai H (2004) Structural basis of long-term potentiation in single dendritic spines. *Nature* 429(6993):761–766.
17. Bastrikova N, Gardner GA, Reece JM, Jeromin A, Dudek SM (2008) Synapse elimination accompanies functional plasticity in hippocampal neurons. *Proc Natl Acad Sci USA* 105(8):3123–3127.
18. Syken J, Grandpre T, Kanold PO, Shatz CJ (2006) PirB restricts ocular-dominance plasticity in visual cortex. *Science* 313(5794):1795–1800.
19. Datwani A, et al. (2009) Classical MHCI molecules regulate retinogeniculate refinement and limit ocular dominance plasticity. *Neuron* 64(4):463–470.
20. Huh GS, et al. (2000) Functional requirement for class I MHC in CNS development and plasticity. *Science* 290(5499):2155–2159.
21. Corriveau RA, Huh GS, Shatz CJ (1998) Regulation of class I MHC gene expression in the developing and mature CNS by neural activity. *Neuron* 21(3):505–520.
22. Feng G, et al. (2000) Imaging neuronal subsets in transgenic mice expressing multiple spectral variants of GFP. *Neuron* 28(1):41–51.
23. Holtmaat AJ, et al. (2005) Transient and persistent dendritic spines in the neocortex in vivo. *Neuron* 45(2):279–291.
24. Oray S, Majewska A, Sur M (2004) Dendritic spine dynamics are regulated by monocular deprivation and extracellular matrix degradation. *Neuron* 44(6):1021–1030.
25. Lendvai B, Stern EA, Chen B, Svoboda K (2000) Experience-dependent plasticity of dendritic spines in the developing rat barrel cortex in vivo. *Nature* 404(6780):876–881.
26. Kirkwood A, Bear MF (1994) Homosynaptic long-term depression in the visual cortex. *J Neurosci* 14(5 Pt 2):3404–3412.
27. Becker N, Wierenga CJ, Fonseca R, Bonhoeffer T, Nägerl UV (2008) LTD induction causes morphological changes of presynaptic boutons and reduces their contacts with spines. *Neuron* 60(4):590–597.
28. Heynen AJ, et al. (2003) Molecular mechanism for loss of visual cortical responsiveness following brief monocular deprivation. *Nat Neurosci* 6(8):854–862.
29. Kirkwood A, Rioult MC, Bear MF (1996) Experience-dependent modification of synaptic plasticity in visual cortex. *Nature* 381(6582):526–528.
30. Schuett S, Bonhoeffer T, Hübener M (2002) Mapping retinotopic structure in mouse visual cortex with optical imaging. *J Neurosci* 22(15):6549–6559.
31. Tagawa Y, Kanold PO, Majdan M, Shatz CJ (2005) Multiple periods of functional ocular dominance plasticity in mouse visual cortex. *Nat Neurosci* 8(3):380–388.
32. Hofer SB, Mrsic-Flogel TD, Bonhoeffer T, Hübener M (2006) Prior experience enhances plasticity in adult visual cortex. *Nat Neurosci* 9(1):127–132.
33. Sato M, Stryker MP (2008) Distinctive features of adult ocular dominance plasticity. *J Neurosci* 28(41):10278–10286.
34. Sawtell NB, et al. (2003) NMDA receptor-dependent ocular dominance plasticity in adult visual cortex. *Neuron* 38(6):977–985.
35. Roberts TF, Tschida KA, Klein ME, Mooney R (2010) Rapid spine stabilization and synaptic enhancement at the onset of behavioural learning. *Nature* 463(7283):948–952.
36. Yang G, Pan F, Gan WB (2009) Stably maintained dendritic spines are associated with lifelong memories. *Nature* 462(7275):920–924.
37. Arellano JI, Benavides-Piccione R, Defelipe J, Yuste R (2007) Ultrastructure of dendritic spines: Correlation between synaptic and spine morphologies. *Front Neurosci* 1(1):131–143.
38. McGee AW, Yang Y, Fischer QS, Daw NW, Strittmatter SM (2005) Experience-driven plasticity of visual cortex limited by myelin and Nogo receptor. *Science* 309(5744):2222–2226.
39. Atwal JK, et al. (2008) PirB is a functional receptor for myelin inhibitors of axonal regeneration. *Science* 322(5903):967–970.
40. Akbik FV, Bhagat SM, Patel PR, Cafferty WB, Strittmatter SM (2013) Anatomical plasticity of adult brain is titrated by Nogo Receptor 1. *Neuron* 77(5):859–866.
41. William CM, et al. (2012) Synaptic plasticity defect following visual deprivation in Alzheimer's disease model transgenic mice. *J Neurosci* 32(23):8004–8011.
42. Kim T, et al. (2013) Human LilrB2 is a β-amyloid receptor and its murine homolog PirB regulates synaptic plasticity in an Alzheimer's model. *Science* 341(6152):1399–1404.